

1 In vitro gastric lipid digestion of emulsions with  
2 mixed emulsifiers: correlation between lipolysis  
3 kinetics and interfacial characteristics

4 *Marcos R. INFANTES-GARCIA<sup>1</sup>, Sarah H.E. VERKEMPINCK<sup>1</sup>, Teresa DEL CASTILLO-SANTAELLA<sup>2,3</sup>,*  
5 *Julia MALDONADO-VALDERRAMA<sup>2,4</sup>, Marc E. HENDRICKX<sup>1</sup>, Tara GRAUWET<sup>1</sup>*

6 <sup>1</sup> Laboratory of Food Technology and Leuven Food Science and Nutrition Research Centre (LFoRCe),  
7 Department of Microbial and Molecular Systems (M2S), KU Leuven, Kasteelpark Arenberg 22, PB 2457,  
8 3001 Leuven, Belgium

9 <sup>2</sup> Department of Applied Physics, University of Granada, Avenida de Fuente Nueva, s/n, Granada C.P.  
10 18071, Spain

11 <sup>3</sup> Department of Physical Chemistry, University of Granada, Faculty of Pharmacy, Cartuja Campus, s/n,  
12 C.P. 18071, Granada, Spain

13 <sup>4</sup> Excellence Research Unit “Modeling Nature” (MNat), University of Granada, Avda. del Hospicio, s/n,  
14 C.P. 18010, Granada, Spain

15

16 **Abstract**

17 Emulsions stabilized by a mixture of emulsifiers may show a tailored functionality depending on the  
18 compatibility of the emulsifiers employed. This was proposed in a previous work dealing with distinct  
19 lipolysis kinetics of citrus pectin (CP) and Tween 80 (TW80) based emulsions. CP provided a fast a high  
20 extent of gastric lipid hydrolysis, TW80 presented negligible digestion and emulsions stabilized with  
21 mixtures presented intermediate lipolysis kinetics. The current research work aimed to investigate the  
22 interfacial mechanisms underlying gastric lipolysis to further understand the encountered behavior on a  
23 fundamental basis. This was achieved by monitoring the interfacial tension kinetics and measuring the  
24 interfacial rheology of interfacial layers during *in vitro* digestion using a modified pendant drop technique.  
25 This allowed the correlation of emulsions *in vitro* lipolysis kinetics and interfacial phenomena during  
26 digestion. Two extremely different interfacial tension kinetics were observed when single layers of CP  
27 versus TW80 and intermediate kinetics were observed for the binary interfacial layers, importantly  
28 correlating with results obtained with emulsions. These findings are discussed in detail and confirm that  
29 competitive adsorption between emulsifiers and lipase (e.g. orogenic displacement) is a key factor  
30 determining the lipolysis kinetics of emulsions stabilized by mixed emulsifiers.

31 **Keywords**

32 Gastric lipase; lipid digestion, orogenic displacement; interfacial tension; interfacial rheology, OCTOPUS.

## 33 **1. Introduction**

34 Oil-in-water (o/w) emulsions are widely spread among commercial food products such as milk, dressings,  
35 soups, sauces, but also among a range of nutraceutical and pharmaceutical products (Bouyer et al., 2012;  
36 McClements, 2018). Rational emulsion property design to obtain a particular functionality has been a recent  
37 trend in the field. Nutritionally speaking, the emulsion lipid phase contributes with the energy and essential  
38 fatty acids provision for our body. Additionally, emulsions allow the encapsulation, protection and transport  
39 of lipophilic compounds, tailoring the delivery inside the gastrointestinal tract (Corstens et al., 2017). In  
40 this aspect, interfacial engineering of o/w emulsions gained increasing interest in recent years in the food  
41 science and technology field. Their interfacial initial properties often determine their physicochemical  
42 stability and/or susceptibility to enzymatic degradation in the gastrointestinal tract (Troise et al., 2020).

43 The emulsion interface needs to be thermodynamically stabilized, otherwise the dispersed oil droplets  
44 undergo different instability phenomena (e.g. flocculation, coalescence, Ostwald ripening). For this reason,  
45 emulsifiers are essential emulsion ingredients normally added to stabilize the oil-water interface. These  
46 emulsifiers can be broadly classified as low-molecular-weight surfactants (e.g. Tweens, phospholipids,  
47 monoglycerides, and others) and amphiphilic biopolymers (e.g.  $\beta$ -lactoglobulin, pectin, and others)  
48 (Berton-Carabin & Schroën, 2019). O/w emulsions can be stabilized by a single type of emulsifier.  
49 Nevertheless, the physicochemical stability and digestive functionality of emulsions can be fine-tuned by  
50 combining emulsifiers, instead of using individual ones (Dickinson, 2011; McClements & Jafari, 2018).  
51 Moreover, mixes of emulsifiers are normally employed in more complex emulsified food products.

52 The emulsion interfacial properties govern the adsorption of lipases to the oil-water interface, and therefore,  
53 determine the lipid digestion kinetics (Berton-Carabin & Schroën, 2019). Three main phenomena are  
54 impacted by the nature of the surface-active compounds adsorbed to the interface: the emulsion physical  
55 stability, competitive adsorption between emulsifiers and lipases, as well as the potential digestion  
56 phenomena taking place at the interface (Singh & Ye, 2013). The first phenomenon is intrinsically related  
57 to the interface. Depending on the nature of the emulsifier stabilizing the interface, this emulsifier may

58 undergo physicochemical changes due to digestive conditions (e.g. acidity, ionic strength) leading to its  
59 desorption from the interface and further emulsion destabilization (Verkempinck, Salvia-Trujillo, Moens,  
60 et al., 2018). This emulsion instability induces changes in the available surface for lipase adsorption which  
61 impacts the kinetics of lipid digestion. The second phenomenon linked to the emulsion interface is the  
62 competitive adsorption between emulsifiers and lipases. If the emulsifiers are strongly adsorbed to the  
63 interface, the access of lipases to the interface can be hindered or even completely inhibited (Scheuble et  
64 al., 2016). In this aspect, there is limited information regarding the impact of emulsions stabilized by a mix  
65 of emulsifiers on their behavior along the gastrointestinal tract. Only few studies assessed the lipid digestion  
66 kinetics of emulsions stabilized by mixed emulsifiers and none of them in the gastric compartment  
67 (Dickinson, 2011; Klinkesorn & McClements, 2009; Li & McClements, 2014; Wulff-Pérez et al., 2010). A  
68 third phenomenon linked to the interfacial composition is the potential hydrolysis of the interfacial layer by  
69 digestion enzymes (Singh et al., 2009). This may occur to surface-active compounds such as proteins,  
70 digestible carbohydrates (e.g. modified starches), and/or digestible lipids (e.g. lecithin, mono- and  
71 diglycerides), but not to other compounds such as tweens or fibers like pectin. The cleavage of these  
72 compounds at the interface mainly affects the emulsion physical stability.

73 In this aspect, there is a research opportunity to describe lipolysis in the gastric phase. Diverse *in vivo*  
74 implications may be triggered by gastric lipid digestion. Gastric lipolysis, although limited, has been  
75 suggested to stimulate pancreatic lipid digestion by causing droplet disruption, increasing the solubilization  
76 of digestion products, promoting hormone release and augmenting colipase (coenzyme) binding capacity  
77 of pancreatic lipase (McClements, Decker, and Park 2008). Lipid digestion in the stomach is also highly  
78 relevant for people suffering of exocrine pancreatic insufficiency (low pancreatic enzymes production)  
79 (Layer & Keller, 2005). Moreover, gastric lipase is an essential enzyme for infant lipid digestion since their  
80 pancreas is not yet fully developed at birth, resulting in a relatively low secretion of pancreatic lipase, while  
81 on the contrary, their HGL expression is already fully mature (Bourlieu et al., 2014; Lindquist & Hernell,  
82 2010).

83 Lipid digestion is considered an interfacial phenomena as lipases have to adsorb at the oil-water interface  
84 in competition with the emulsifiers in order to access the oil and hydrolyze triacylglycerols into fatty acids  
85 and monoglycerides. Thus, interfacial changes in emulsion along the gastrointestinal tract play a very  
86 important role during lipid digestion (Maldonado-Valderrama, 2019). Two important interfacial properties  
87 that can be monitored during *in vitro* digestion are the interfacial tension and interfacial rheology. These  
88 properties are indicators of the interactions between the initially adsorbed emulsifiers, bile salts and lipases.  
89 One important interaction among these elements is the displacement of emulsifiers by bile salts and/or  
90 lipases. Most lipid digestion studies have characterized interfacial layer changes during the small intestinal  
91 phase since it is the compartment where lipids are majorly digested (Aguilera-Garrido et al., 2021; Corstens  
92 et al., 2017; Macierzanka et al., 2009; Maldonado-Valderrama et al., 2013; Wei et al., 2021). This work  
93 shows for the first time, mixed interfacial layers composed of a small surfactant and biopolymer subjected  
94 to *in vitro* gastric digestion in presence of a relevant substitute of gastric lipase. In the gastric phase, only  
95 one study have monitored the interfacial tension kinetics during *in vitro* gastric lipid digestion (Scheuble et  
96 al., 2016). Therefore, there are research opportunities to obtain insights on the interactions between  
97 emulsifiers and gastric lipase.

98 In our previous work, diverse emulsions stabilized by a single emulsifier were subjected to *in vitro* gastric  
99 digestion (Infantes-Garcia, Verkempinck, Gonzalez-Fuentes, et al., 2021). From these experiments, citrus  
100 pectin (CP)- and Tween 80 (TW80)-based emulsions showed distinct physical stability and lipolysis  
101 kinetics under simulated gastric conditions. Substantial amount of research has demonstrated the interfacial  
102 activity (capacity to adsorb onto oil-water interfaces) of certain types of pectin (Humerez-Flores et al.,  
103 2021, 2022; Neckebroek et al., 2020; Verkempinck, Kyomugasho, et al., 2018; Verkempinck, Salvia-  
104 Trujillo, Denis, et al., 2018; Wei et al., 2021). More specifically, the CP-based emulsion exhibited a  
105 moderate physical stability and high lipolysis extent, while the TW80-based emulsion a high stability but  
106 negligible lipolysis extent. For that reason, we mixed these two stabilizing agents with the objective of  
107 forming emulsions with both of them adsorbed to the interface exhibiting a complementary functionality.

108 In our most recent work, the *in vitro* gastric lipolysis behavior was modulated by emulsions with mixed  
109 interfaces (Infantes-Garcia et al., 2022). A competitive adsorption phenomenon was hypothesized to  
110 explain the detected lipolysis kinetics modulation. Accordingly, the objective of this research was to  
111 specifically design and *in vitro* digest interfaces stabilized by single versus mixed interfaces, and correlate  
112 their interfacial tension behavior with the lipid digestion trends observed in our previous studies. Section  
113 3.1 of the results and discussion part compiles and merges the most interesting findings of our two previous  
114 studies regarding some emulsion physical stability indicators and *in vitro* gastric lipolysis behavior. Section  
115 3.2 discusses the interfacial characterization of single and mixed interfacial layers during *in vitro* gastric  
116 digestion in which a correlation with the lipolysis kinetics is also included. These interfacial layers were  
117 characterized in terms of interfacial tension kinetics and interfacial dilatational rheology, which allowed us  
118 to obtain insight into the competitive adsorption phenomenon. These interfacial layers were characterized  
119 in terms of interfacial tension kinetics and interfacial dilatational rheology, which allowed us to obtain new  
120 insight into the composition of the interface and the interfacial interactions.

## 121 **2. Experimental methods**

### 122 **2.1 Production of o/w emulsions**

123 Triolein (> 99 %, Acros Organics, Geel, Belgium) was utilized as oil phase since different commercial  
124 plant-based oils such as olive, canola or sunflower oil are rich in this triglyceride (Karupaiah & Sundram,  
125 2007). Citrus pectin (CP, degree of methylesterification  $\geq$  85 %, Sigma-Aldrich, Diegem, Belgium) and  
126 Tween 80 (TW80, Sigma-Aldrich, Diegem, Belgium) were utilized as emulsifying agents. Since one of the  
127 objectives in this research was to form emulsions with mixed interfaces, the difference in surface activity  
128 of CP and TW80 should be considered as interesting rationale for their combined selection. For instance, it  
129 is well known that large molecules, like CP, adsorb at a slower rate than small surfactants such as TW80  
130 (McClements, 2016). For this reason, it was decided to follow a post-homogenization procedure to prepare  
131 the emulsions with mixed interfaces. Firstly, an emulsion stabilized by CP was prepared, and secondly, this

132 emulsion was mixed with a TW80 solution. This strategy permitted the formation of mixed interfacial layers  
133 without the total desorption of CP (McClements & Jafari, 2018).

134 The coarse CP emulsions were produced with a high-shear mixer (Ultra-Turrax T25, IKA, Staufen,  
135 Germany) at 13500 rpm for 5 min, to obtain emulsions consisting of triolein (10 % w/w), CP (2 % w/w)  
136 and ultrapure water (88 % w/w). Afterwards, the coarse emulsions were homogenized in a high-pressure  
137 homogenizer (Stansted Fluid Power, Pressure cell homogenizer, U.K.) at 100 MPa (one cycle). Next to the  
138 homogenization step, each CP emulsion was mixed with one of the two TW80 solutions in a ratio 1:1  
139 resulting in contents of 5% of triolein, 1% of CP, and TW80 concentrations of 0.00625 or 0.1 %. The level  
140 of 1% CP was chosen because it generated a stable emulsion without significantly increasing the bulk  
141 viscosity (Verkempinck, Salvia-Trujillo, Denis, et al., 2018). These mixtures were gently stirred for 1 h.  
142 For the emulsions stabilized by a single emulsifier (CP or TW80), the same mixing and homogenization  
143 conditions explained above were applied. The pH of all emulsions containing CP was around 2.7, while the  
144 TW80 emulsion exhibited a pH around 6.8. On the one hand, the low pH of the emulsions containing CP  
145 was due to the acid extraction process of pectin. On the other hand, TW80 production process does not  
146 require strong acids or alkalis, and thus the pH of the emulsion was close to neutrality. Even if these values  
147 are largely different from each other, during *in vitro* gastric digestion, the pH is adjusted to 3. At that pH,  
148 CP emulsions present a relatively good physical stability, while TW80 is unaffected by acid pH values.

## 149 **2.2 *In vitro* gastric digestion of the generated emulsions**

150 The static *in vitro* INFOGEST protocol was employed to analyze the kinetics of gastric lipolysis of the  
151 generated emulsions (Brodkorb et al., 2019). In this case, a scaled-down version of the INFOGEST protocol  
152 was employed exactly as described in our previous work (Infantes-Garcia, Verkempinck, Gonzalez-  
153 Fuentes, et al., 2021). In this aspect, a gastric lipase activity of 60 U/mL (tributyryl-based) was set in the  
154 gastric phase performed at pH 3 (Grundy et al., 2021). The gastric lipid digestion kinetics were evaluated  
155 by digesting independent samples (tubes) as a function of time (5; 10; 15; 30; 45; 60; 90; 120 min after

156 enzyme addition). Lipolysis was stopped through chemical inhibition (10  $\mu$ L of Orlistat 100 mM in  
157 ethanol).

### 158 **2.3 Monitoring of oil droplet characteristics during *in vitro* gastric digestion**

159 Additional chyme samples were generated at 4 different gastric digestion moments (after 15; 30; 60 and  
160 120 min in the gastric phase) in an independent experiment and their oil droplet characteristics were  
161 determined (i.e. particle charge, microstructure, and particle size).

162 **Microstructure:** Microstructural visualization of oil droplets was carried out using an optical microscope  
163 (Olympus BX-41) fitted with an Olympus XC-50 digital camera (Olympus, Opticel Co. Ltd., Tokyo, Japan)  
164 at 40x magnification (Infantes-Garcia et al., 2020).

165 **Particle size:** The particle size of all samples was determined employing a laser diffraction equipment  
166 (Beckman Coulter Inc., LS 13 320, FL, USA). All equipment parameters were set as explained in our  
167 previous work (Infantes-Garcia, Verkempinck, Gonzalez-Fuentes, et al., 2021).

168 **Particle charge:** The  $\zeta$ -potential of oil droplets was measured using a dynamic light scattering  
169 electrophoresis equipment (Zetasizer NanoZS, Malvern Instruments, Worcestershire, UK). Emulsions or  
170 chyme samples were diluted in a ratio 1:10 with pure ultrapure water or ultrapure water adjusted to pH 3,  
171 respectively (Infantes-Garcia, Verkempinck, Gonzalez-Fuentes, et al., 2021).

### 172 **2.4 Analysis of lipid digestion products**

173 An HPLC-charged aerosol detector method was employed to quantify triolein (TAG) and its hydrolysis  
174 products diolein (DAG), monoolein (MAG) and oleic acid (FFA). Lipids were extracted and quantified  
175 according to our previous work which is briefly described below (Infantes-Garcia, Verkempinck, Guevara-  
176 Zambrano, et al., 2021).

#### 177 2.4.1 Extraction of lipids

178 In sum, 1 mL of sample was placed in a glass tube together with 0.2 mL sulphuric acid (2.5 M), 2 mL  
179 ethanol, and 3 mL diethylether:heptane (DEE:H=1:1). The tube was vortexed for 2 min, followed by an  
180 end-over-end rotation at 15 rpm for 30 min. Afterwards, the upper non-polar layer was collected in a 5 mL  
181 volumetric flask. A second extraction was done by addition of 1 mL of DEE:H into the previous tube,  
182 vortexed for 2 min, and mixed in an end-over-end rotator at 15 rpm for 15 min. The upper layer was  
183 collected in the same volumetric flask, which was brought to 5 mL by adding DEE:H. The lipid extract was  
184 filtered (Chromafil PET filters, 0.20  $\mu$ L pore size, 25 mm diameter) and stored at  $-80$  °C until analysis.

#### 185 2.4.2 Chromatographic lipid quantification

186 The extracted lipids were injected in an HPLC system (Agilent Technologies 1200 Series, Diegem,  
187 Belgium) fitted with a silica column (Chromolith Performance Si, 100–4.6 mm, Merck, Darmstadt,  
188 Germany) preserved with a guard column (Merck, Darmstadt, Germany). An external oven (Chromaster  
189 5310, VWR, Hitachi Ltd., Tokyo, Japan) was used to keep the column temperature at 40 °C. Lipids species  
190 were separated by a quaternary gradient: isooctane (solvent A), acetone:ethyl acetate (2:1 v/v) containing  
191 0.02% (v/v) of acetic acid (solvent B), isopropanol:water (85:15 v/v) containing 0.5% (v/v) of acetic acid  
192 and triethylamine (solvent C), and isopropanol (solvent D). Detection was performed in a charged aerosol  
193 detector (Corona Veo, Thermo Fisher Scientific, Geel, Belgium), operated with a gas pressure of 5.5 bar  
194 and evaporator temperature of 35 °C. Calibration curves were constructed using lipid standards and  
195 employed to quantify lipolysis products.

196 Glycerol (GLY) and residual triolein were calculated per digestion time as indicated by (Infantes-Garcia et  
197 al., 2020). In sum, a molar balance based on the sequential lipolysis reactions sequential starting from  
198 triolein was performed to calculate the residual triolein and glycerol.

### 199 **2.5 Interfacial characterization**

200 In a separate experiment, the characterization and *in vitro* digestion of single versus mixed interfaces  
201 composed of CP and/or TW80 was performed using the OCTOPUS: a pendant drop film balance equipped

202 with a multisubphase exchange system which is described in detail elsewhere (JMaldonado-Valderrama et  
203 al., 2013; Maldonado-Valderrama, 2019). In this equipment, a single aqueous solution droplet was formed  
204 at the tip of a double capillary directly immersed in the oil phase, kept in a heated (37 °C) cuvette  
205 (Hellma®). The OCTOPUS allows the online measurement of the interfacial tension kinetics and the  
206 interfacial dilatational rheology as surface-active compounds adsorb onto the oil-water interface. The  
207 software packages DINATEN© and CONTACTO© were employed to measure the interfacial tension and  
208 interfacial dilatational rheology data, respectively. Images of the drop were taken as function of time by a  
209 charge-coupled camera (Pixelink®) Experimental drop profiles were extracted and fitted to the Young-  
210 Laplace equation to determine the volume, surface tension, and the interfacial area of the pendant drop  
211 through Axisymmetric Drop Shape Analysis (ADSA). The equipment uses a fuzzy logic area control to  
212 maintain the interfacial area constant during the experiment. After stabilizing, or *in vitro* digesting, the  
213 interfacial layer at constant interfacial area (20 mm<sup>2</sup>), volume oscillations of the drop were applied to  
214 evaluate the dilatational viscoelasticity of the interfacial layer. The dilatational modulus ( $E$ ) of the  
215 interfacial layer is defined by a real and an imaginary component:

$$216 \quad 2.6 \quad E = E' + iE'' = \varepsilon + i\eta\nu \quad (1)$$

217 In equation (1), the term  $E'$  is the storage modulus that accounts for the interfacial elasticity ( $\varepsilon$ ), while  $E''$   
218 is the loss modulus accounting for the interfacial viscosity ( $\eta$ ) of the adsorbed layer and  $\nu$  is the angular  
219 frequency of the oscillation. The oscillation amplitude was maintained below 5% variation to assure linear  
220 regime and the oscillation frequency was set to 0.1 Hz. At this relatively high frequency (0.1 Hz), the  
221 dilatational rheology will be mainly elastic and the dilatational modulus can be approximated by the storage  
222 modulus or interfacial elasticity as the viscosity or loss modulus can be neglected (results not shown)  
223 (Maldonado-Valderrama et al., 2005). The dilatational elasticity contains information about the inter- and  
224 intramolecular associations at the interfacial layer and provide information on the composition of the  
225 interfacial layer (Aguilera-Garrido et al., 2021). Also, at 0.1 Hz, the dilatational response highlights  
226 differences between proteins, who develop a cohesive layer with high elasticity and surfactants, which

227 develop a more mobile and fluid interface with lower  $E$ , also allowing comparison with other experimental  
228 works (Maldonado-Valderrama & Patino, 2010).

229 In the OCTOPUS, the normal capillary is substituted by a double capillary which allows simultaneous  
230 injection and extraction of liquid from the droplet (Cabrerizo-Vílchez et al., 1999). This allows a subphase  
231 exchange of the bulk and simulating the digestive process in a single droplet, as explained in detail  
232 elsewhere (Maldonado-Valderrama et al., 2013; Maldonado-Valderrama, 2019). Single and mixed  
233 interfacial layers were formed and subjected to *in vitro* gastric conditions through subphase exchange of  
234 the droplet bulk solution with gastric media.

235 The oil phase was high-oleic sunflower oil (~70% oleic acid), kindly donated by Vandemoortele (Ghent,  
236 Belgium). It was employed in this independent experiment due to technical reasons. However, this oil  
237 presents a very high triolein content which makes it suitable as a replacement of pure triolein. This oil was  
238 previously purified with Florisil resins (oil:Florisil 2:1) reaching an interfacial tension of ~30 mN/m in  
239 ultrapure water (Maldonado-Valderrama et al., 2013). In case of the single interfacial layers, either 1% CP  
240 or TW80 solutions were utilized to form drops and allow the adsorption of the surface-active compounds.  
241 For the mixed interfacial layers, a two-step interfacial layer formation was followed by first forming a drop  
242 containing 1% CP, permitting the biopolymer to adsorb. Afterwards, solutions containing 0.00625 or 0.1%  
243 TW80 were pumped and replaced the droplet bulk solution allowing the formation of a mixed interfacial  
244 layer. After stabilization of these single or mixed interfacial layer, they were subjected to *in vitro* gastric  
245 digestion by replacing again the bulk solution with simulated gastric media by means of subphase exchange.  
246 We intended to simulate the digestive conditions as close as possible as in the *in vitro* digestion protocol  
247 for o/w emulsions previously described. For this purpose, a simulated gastric fluid (SGF) adjusted to pH 3  
248 containing electrolytes and a rabbit gastric extract (60 U/mL tributyrin-based) was utilized as recommended  
249 by the international network INFOGEST (Brodkorb et al., 2019). The *in vitro* gastric digestion of the  
250 interfacial layers was carried out for 2 hours at constant interfacial area of 20 mm<sup>2</sup> (by slightly varying the  
251 droplet volume). As a final step, the droplet bulk solution is exchanged with water to force desorption of

252 emulsifiers and soluble products of digestion. This exchange depletes the bulk solution of material leaving  
 253 a mixture of lipophilic digestive products at the interface and undigested emulsifier. In the case of TW80,  
 254 the SGF contained also enough concentration of TW80 to avoid spontaneous desorption owing to depletion  
 255 of TW80 in the bulk solution. A final desorption step consisting of subphase exchange of droplet bulk  
 256 solution by a simulated gastric fluid, which depletes the bulk of soluble products of lipolysis and allows  
 257 evaluating the presence of lipolytic digestive products at the interface (Maldonado-Valderrama, 2019). The  
 258 interfacial tension was simultaneously monitored throughout the whole simulated digestion and the  
 259 interfacial rheology was measured at the end of each adsorption/desorption step.

## 260 **2.7 Statistical analysis and modeling**

### 261 **2.6.1 One-way ANOVA and comparison test**

262 The oil droplet size,  $\zeta$ -potential during *in vitro* gastric digestion and interfacial properties were statistically  
 263 compared with one-way ANOVA and Tukey HSD comparison analyses ( $P < 0.05$ ) using the statistical  
 264 software JMP (JMP pro14, SAS Institute Inc., Cary, NC, USA).

### 265 **2.6.2 Single-response kinetic modeling**

266 Single-response modeling was employed to compare the lipid hydrolysis behavior of emulsions stabilized  
 267 by single versus mixed interfaces. The selected response for this analysis was the lipid hydrolysis  
 268 percentage (%HYD), which refers to the number of cleaved ester bonds with respect to the total number of  
 269 ester bonds available. This response is described in equation (2):

$$270 \quad \%HYD(t) = \frac{n_{FFA(t)}}{(n_{TAG(t)} \times 3 + n_{DAG(t)} \times 2 + n_{MAG(t)} + n_{FFA(t)})} \quad (2)$$

271 %HYD( $t$ ) is the hydrolysis percentage as a function of gastric digestion time  $t$ ;  $n_{FFA(t)}$ ,  $n_{TAG(t)}$ ,  $n_{DAG(t)}$ , and  
 272  $n_{MAG(t)}$  are the number of moles of oleic acid, residual triolein; diolein, and monoolein, respectively.

273 Data sets were analyzed by means of the software JMP (JMP pro14, SAS Institute Inc., Cary, NC, USA).  
274 After a model discrimination process, the best fit was obtained for the modified Gompertz equation  
275 (Zwietering et al., 1990), which is indicated below in equation (3).

$$276 \quad \%HYD(t) = HYD_f \exp \left\{ - \exp \left[ \frac{k \exp(1)}{H_f} (t_{lag} - t) + 1 \right] \right\} \quad (3)$$

277 The parameter  $\%HYD(t)$  is the percentage hydrolyzed lipids at a time  $t$  (min);  $HYD_f$  (%) is the extent of  
278 the hydrolyzed lipids ( $t = \infty$ );  $k$  ( $\text{min}^{-1}$ ) is the reaction rate constant; and  $t_{lag}$  (min) is the lag time prior lipid  
279 hydrolysis.

### 280 **3. Results and discussion**

#### 281 **3.1 Oil droplet properties and *in vitro* gastric lipid digestion of emulsions formed** 282 **with CP and/or TW80**

283 All prepared emulsions were characterized in terms of oil droplet properties (particle charge,  
284 microstructure, and particle size) and lipolysis product content.

##### 285 **3.1.1. Oil droplet properties**

286 The CP-based emulsion (pH  $\sim$ 2.7) presented an initial negative  $\zeta$ -potential (-20.1 mV). This negative  
287 magnitude is possibly linked to the presence of ionized carboxylic groups in the CP molecule  
288 (Ngouémazong et al., 2015). The  $\zeta$ -potential of CP-based emulsion changed to slightly positive values at  
289 the end of gastric digestion. This is possibly due to charge neutralization of pectin and the presence of  
290 ionized fatty acids generated as a result of lipolysis. The CP-based emulsion exhibited an increase in  
291 average particle size from 1.1 to around 4  $\mu\text{m}$  (Figure 1). The micrographs in Figure 1 revealed that a certain  
292 extent of flocculation and coalescence led to this increase in particle size. In case of the TW80-based  
293 emulsion, a neutral particle charge was expected due to the non-ionic nature of TW80. However, it  
294 presented a slightly negative particle charge of -1.4 mV. This magnitude possibly reflected a certain extent

295 of contamination by fatty acids impurities (Chang & McClements, 2016). When the TW80-based emulsion  
296 was subjected to *in vitro* gastric digestion, the  $\zeta$ -potential did not significantly change which may be an  
297 indication of a limited production of fatty acids. The physical stability of the TW80-based emulsion did not  
298 change during *in vitro* digestion (Figure 1).

299 In case of the emulsions stabilized by mixed interfaces, the  $\zeta$ -potential values laid in between the ones of  
300 emulsions stabilized by CP or TW80 (Table 1). In this aspect, an inverse relation can be observed between  
301 the TW80 concentration and the particle charge. This inverse relation between particle charge and TW80  
302 concentration might be an indication of the increased presence of TW80 at the interface due to CP  
303 displacement. Therefore, interfaces containing both CP and TW80 at different proportions were possibly  
304 created. This latter hypothesis will be further discussed in Section 3.2 (interfacial study). The magnitude of  
305 the  $\zeta$ -potential for the emulsion containing 0.00625% TW80 retained a more negative value after gastric  
306 lipolysis compared to the one of 0.1% TW80. This could be due to the formation a mixed layer composed  
307 of TW80 compressing the interfacial network formed by CP which remained to a large extent at the  
308 interfacial layer. Conversely, the magnitude of the  $\zeta$ -potential for the emulsion containing 0.1% TW80  
309 diminished to a similar value to the one obtained after gastric lipolysis of the emulsion stabilized by TW80  
310 only (Table 1). This is indicative for the predominant presence of TW80 at the interface even when mixed  
311 with CP. In this latter case, CP seemed to be largely displaced from the emulsion interface. Emulsions  
312 stabilized by mixed interfaces showed an improved physical stability compared to a CP-based emulsion  
313 (Figure 1). This phenomenon most likely occurred because TW80 is a non-ionic surfactant. Therefore,  
314 TW80 molecules did not present electrostatic interactions with the ionic CP molecules allowing  
315 compatibility between both surface-active compounds (Guzmán et al., 2016).

### 316 **3.1.2. *In vitro* gastric lipolysis behavior**

317 The percentage of lipid hydrolysis was utilized to compare the *in vitro* digestion behavior of the generated  
318 emulsions by means of single-response modeling (modified Gompertz equation). The representation of the  
319 single-response modeling is given in Figure 2, while the estimated parameters are presented in Table 2.

320 Single-response modeling was not applied to the TW80 data set because it showed a static trend and very  
321 low extent of lipid hydrolysis.

322 The lag time  $t_{lag}$  is defined as the period before the response starts to significantly increase in magnitude.  
323 For the emulsions stabilized by only CP, and by CP and a 0.00625% TW80; this lag time was limited  
324 (Figure 2) as values between 7.7 and 8.2 min were estimated by single-response modeling (Table 2). This  
325 suggests that the interfaces stabilized by the previous single or combined compounds did not represent a  
326 barrier for the (rapid) adsorption of gastric lipase allowing lipid cleavage from the first minutes of digestion.  
327 In Figure 2, it can be observed that the emulsion containing 1% CP and 0.1% TW80 presented a  
328 considerable lag phase with an estimated duration of  $16.8 \pm 2.1$  min. This finding may be related to the higher  
329 interfacial concentration of TW80. TW80 is known to be a surfactant with a high surface activity, thus  
330 gastric lipase probably competed for the interface with CP molecules. Therefore, we hypothesize that the  
331 lag phase might be correlated to the competitive adsorption phenomenon between lipase and CP molecules  
332 since TW80 molecules cannot be desorbed by gastric lipase.

333 The reaction rate constant  $k$  indicates the maximum rate with which the final extent of digestion is obtained.  
334 In this aspect, there was a clear effect on this kinetic parameter if a high TW80 concentration (0.1%) is used  
335 during emulsion preparation. As observed in Table 2, the  $k$  magnitude for this latter emulsion ( $0.19 \text{ min}^{-1}$ )  
336 was significantly lower compared to the other two emulsions ( $0.86 \text{ min}^{-1}$ ). The rate constant is highly  
337 influenced by amount of gastric lipase adsorbed to the interface (McClements, 2018). Therefore, the  
338 emulsion containing 0.1% TW80 probably permitted a lower interfacial concentration of gastric lipase as  
339 compared to the other emulsions. As explained above, a higher concentration of TW80 at the emulsion  
340 interface most probably caused a stronger competitive adsorption phenomenon between gastric lipase and  
341 the initial emulsifiers. As a consequence, a lower lipase interfacial concentration was most likely reached  
342 for this emulsion.

343 Regarding the extent of lipid hydrolysis  $HYD_f$ , this kinetic parameter was also affected by the TW80  
344 concentration in the initial emulsion. A high concentration of this non-ionic surfactant provoked a lower

345 extent of gastric lipid hydrolysis. During gastric digestion, a product inhibition phenomenon can limit the  
346 lipase action through the entrapment of the enzyme by lipolysis products (Pafumi et al., 2002). When a  
347 certain critical concentration of lipolysis products is reached, these products surround gastric lipase and  
348 restrict the access to the triglyceride core. Since the emulsion interface formed with 0.1% TW80 possibly  
349 permitted a low degree of gastric lipase adsorption, gastric lipase was entrapped faster because a lower  
350 concentration of lipolysis products was needed. Therefore, the lipid hydrolysis extent for this emulsion was  
351 much lower compared to the emulsions with no or low amounts of TW80. In case of the TW80-based  
352 emulsion, a negligible extent of digestion was obtained probably because this surfactant formed a compact  
353 interfacial layer which restricted gastric lipase adsorption as also observed by other researchers (Couédelo  
354 et al., 2015; Infantes-Garcia, Verkempinck, Gonzalez-Fuentes, et al., 2021).

355 Since particle size was similar for all emulsions containing CP during *in vitro* gastric digestion, then  
356 emulsion physical stability was not the predominant factor impacting the lipolysis kinetics. Small  
357 differences in initial particle size are there but that these level of differences have not been linked to different  
358 digestion kinetics before (Infantes-Garcia et al., 2022). At this point, we can hypothesize that competitive  
359 adsorption between gastric lipase and the surface-active compounds at the interface possibly played a  
360 crucial role in the modulation of the lipolysis kinetics. Therefore, it is necessary to study the lipid digestion  
361 from an interfacial perspective. This interfacial approach is explored in the following section 3.2 to prove  
362 the intermediate hypotheses established in this section.

### 363 **3.2 Interfacial study of single versus mixed interfaces during *in vitro* gastric** 364 **digestion**

365 As previously discussed, the lipolysis kinetics during *in vitro* gastric digestion could be modulated by  
366 designing emulsions stabilized by CP and TW80 at different ratios. This second part aims to obtain insights  
367 into the interfacial phenomena taking place during *in vitro* gastric digestion. In this aspect, a mixed interface  
368 composed of CP and TW80 has been created and subjected to *in vitro* gastric digestion. The OCTOPUS  
369 equipment allowed the evaluation of the adsorption kinetics and interfacial rheology by means of a modified

370 pendant drop technique. In this equipment, a water drop containing the compound(s) of interest is formed  
371 inside the oil phase. First, interfaces were formed using a similar approach as for the emulsions previously  
372 evaluated: Single interfaces of CP or TW80 were formed in one step. Mixed interfaces in two sequential  
373 steps by saturating the interface with CP and then allowing TW80 adsorption. Second, the formed interfaces  
374 were exposed to *in vitro* gastric conditions including a relevant gastric lipase source (i.e. rabbit gastric  
375 extract).

### 376 **3.2.1 Formation of interfaces**

377 This sub-section describes the process of single and mixed interfacial layers formation and its  
378 characterization in terms of interfacial tension and interfacial rheology.

379 **Single interfaces:** Figure 3A-B shows the adsorption kinetics of CP (blue experimental points) and TW80  
380 (orange experimental points), respectively. Both compounds were able to decrease the interfacial tension  
381 of the oil-water interface (initial value of 30 mN/m) as depicted in Figure 4A. However, it can be observed  
382 in Figure 3 that the biopolymer CP has a slower adsorption rate compared to the surfactant TW80. In  
383 addition, TW80 reduced the interfacial tension to lower values (6 mN/m) than CP (15 mN/m). These  
384 findings are coherent since the CP (60 kDa) is a larger molecule compared to TW80 (1.2-1.3 kDa) (Gomes  
385 et al., 2018; Ngouémazong et al., 2015). This result can be interpreted as a higher surface activity of the  
386 TW80 molecules as compared to CP, which can be related to the adsorption mechanism of these  
387 compounds. On the one hand, TW80 molecules contain a carbon chain of oleic acid, which may facilitate  
388 the anchoring of this surfactant to the oil phase (Gomes et al., 2018). On the other hand, CP molecules  
389 contain hydrophobic groups, such as protein moieties, which serve as anchor sites to the oil phase, while  
390 the largest part corresponds to the hydrophilic polysaccharide units which orient towards the aqueous phase  
391 (Ngouémazong et al., 2015). A small fraction of proteins chemically bound (~2 %) to pectin is normally  
392 co-extracted as previously quantified in our research unit (Kyomugasho et al., 2017). Other studies showed  
393 comparable interfacial tension kinetics for CP or TW80 at the same concentrations (Gomes et al., 2018;  
394 Verkempinck, Kyomugasho, et al., 2018). The interfacial activity of CP has also been proven in our

395 previous work, in which the interfacial composition of emulsions prepared with 1% CP was determined.  
396 This was possible through the use of a centrifugation step followed by the quantification of CP via a specific  
397 spectrophotometric method (Infantes-Garcia et al., 2022). We proved that pectin was adsorbed to the oil-  
398 water interface of emulsions.

399 An interesting result to highlight is the significantly different viscoelastic behavior of the CP and TW80  
400 interfacial layers as observed in Figure 4B. The interfacial layer composed of CP presented an elastic  
401 modulus of 82 mN/m, while the one stabilized by TW80 a value of 6 mN/m at 0.1 Hz. At this relatively  
402 high frequency the viscous modulus is negligible ( $E''=0$ ) and the interfacial layers are mainly elastic where  
403 the dilatational modulus coincides with the elastic modulus ( $E=E'$ ) (results not shown). This result reflects  
404 the formation of a compact layer of CP, with highly interconnected molecules. This interfacial network is  
405 composed of irreversibly adsorbed CP (data not shown), displaying similar values to globular protein  
406 interfacial layers measured at similar frequency (Maldonado-Valderrama et al., 2013).  
407 Adsorption/desorption steps of interfaces formed by CP without including a digestion step confirmed that  
408 this biopolymer was irreversibly adsorbed (data not shown). The elastic behavior of CP at the interface can  
409 be related to the number of hydrogen bonds that are formed among the CP molecules. Other authors found  
410 a dilatational elastic modulus of 60 mN/m for a CP layer adsorbed to a rapeseed oil-water interface (Schmidt  
411 et al., 2017). This value is slightly lower than obtained in the present study, most probably this is related to  
412 the differences in structural characteristics of CP among the two studies. In case of TW80, the low  
413 dilatational elasticity, obtained even at this high frequency, indicates the formation of a fluent, mobile  
414 interfacial film and is consistent with values of soluble surfactants which reversibly adsorb at the interface  
415 (Mackie et al., 2001). Consequently, CP showing a high viscoelasticity stabilizes emulsions by the  
416 formation of a cohesive viscoelastic network at the interface which resists deformation. The surfactant  
417 TW80 stabilizes emulsions by the Gibbs-Marangoni mechanism based on the formation of fluid and mobile  
418 films with high surface activity. Measurements of dilatational rheology at this frequency of oscillation allow  
419 differentiating between the two types of interfacial layers formed by CP and TW80 and was therefore used

420 hereafter to evaluate changes in the interfacial composition of the mixtures (Maldonado-Valderrama &  
421 Patino, 2010).

422 **Mixed interfaces:** Figures 3C-D illustrates the interfacial tension kinetics during the formation of mixed  
423 interfaces containing both CP and TW80. This strategy consisted in a sequential adsorption of these two  
424 surface-active agents. As observed in Figures 3C and D, an interfacial layer saturated by CP was first  
425 formed followed by the adsorption of TW80 which was tested at two concentrations (0.00625 versus 0.1%).  
426 Both concentrations were above the critical micellar concentration of TW80 (~0.003%) (Bał & Podgórska,  
427 2016). However, distinct adsorption kinetics were observed after TW80 was injected into the system at the  
428 concentrations tested. In case of the lower concentration (0.00625%), a gradual adsorption of TW80  
429 molecules was observed leading to a slight decrease in interfacial tension from around 16 to 14 mN/m as  
430 depicted in Figure 4A. The higher TW80 concentration (0.1%) resulted in a faster and significant lower  
431 interfacial tension value (decrease from 16 to 9 mN/m). These different behaviors can be attributed to the  
432 phenomenon known as orogenic displacement, discussed in the following paragraph.

433 The orogenic displacement mechanism was proposed after studying oil-water mixed interfaces composed  
434 of milk proteins (biopolymer) and Tween 20 (surfactant) by means of atomic force micrographs and surface  
435 tension measurements (Mackie et al., 2000). As explained by Mackie et al. (1999), this phenomenon  
436 consists of three main steps after the formation of a biopolymer interfacial layer. *(i)* First, minor domains  
437 of surfactant are formed within the interface due to the presence of small defects in the biopolymer film.  
438 This does not affect the original interfacial layer formed by the polymer. *(ii)* Second, when the surfactant  
439 concentration increases, the domains containing the surfactant grow. This causes a disturbance of the  
440 biopolymer interfacial layer leading to a partial displacement from the interface. *(iii)* Third, as the surfactant  
441 concentration keeps on increasing, the biopolymer layer collapses and is completely removed from the  
442 interface (Alan R. Mackie et al., 1999). Therefore, the orogenic displacement mechanism suggests that the  
443 disturbance and potential displacement of the biopolymer film by the surfactant depends on the surfactant  
444 concentration.

445 Based on our findings, an orogenic displacement phenomenon can also explain the behavior of the mixed  
446 interfaces formed by CP and TW80. For instance, in case of the mixed interfacial layer formed after the  
447 addition of TW80 in low concentrations (0.00625%), TW80 possibly adsorbed onto small defects at the CP  
448 interfacial layer. The presence of low concentrations of the highly surface active TW80 at the interfacial  
449 layer slightly reduces the final interfacial tension (Figure 4A), but drastically affects the dilatational  
450 elasticity as TW80 molecules disrupted the interfacial network and interconnection between adsorbed CP  
451 molecules (Figure 4B). Possibly, the interfacial layer is composed of small spots of TW80 compressing the  
452 interfacial network of CP, which probably remains at a relatively high extent at the interface. As a  
453 consequence, no or limited displacement took place and the interfacial tension decreased only to a slight  
454 extent. The  $\zeta$ -potential measurement of the emulsion in Table 1 also indicated a similar behavior (no or  
455 limited CP displacement). However, the presence of TW80 at the interfacial layer caused a significant  
456 decrement in the interfacial elastic modulus reaching a magnitude of 37 mN/m (Figure 4B). This means  
457 that the elasticity of the initial CP film (90 mN/m) was diminished as TW80 molecules disturbed the  
458 intermolecular CP interactions, more specifically the hydrogen bonds among CP molecules. It can be  
459 hypothesized that in case of the addition of 0.00625% TW80, only the first phase of orogenic displacement  
460 occurs. As the TW80 concentration increased to 0.1%, the adsorbed TW80 regions probably grew and  
461 provoked displacement of CP from the interface. In this case, the interfacial elastic modulus decreased from  
462 87 to 11 mN/m (Figure 4B), proving that the elastic network of CP at the interface was seriously damaged  
463 and the interfacial layer contained large regions of TW80. It must be noted that a complete displacement of  
464 CP molecules most likely did not occur since the interfacial layer presented a slightly higher elastic behavior  
465 (11 mN/m) as compared to the single TW80 film (6 mN/m). Hence revealing the anchoring of some CP  
466 molecules to the interfacial layer, although incapable of creating an interconnected network. Thus, the  
467 interfacial characterization indicated that mixed interfacial layers were successfully created.

468 In our previous work, the interfacial composition of emulsions prepared with 1% CP, and 0.1 or 0.00625%  
469 TW80 was determined using a centrifugation step followed by the quantification of CP and TW80 (Infantes-

470 Garcia et al., 2022). We proved that a mixed interfacial layer could be formed in the emulsion. In addition,  
471 it was observed that higher TW80 concentrations used to prepare the emulsions led to a higher degree of  
472 CP desorption from the interface. In the current research, the formation of these mixed layers using the  
473 pendant drop technique showed that as the concentration of TW80 increased, the interfacial layer of CP  
474 was compressed and/or desorb from the interface. This finding can also be linked to the interfacial  
475 composition determination in our previous work (Infantes-Garcia et al., 2022). The interfacial layer evolved  
476 from a CP dominated cohesive interconnected network to a TW80 dominated fluid film, stabilizing  
477 emulsions by the Gibbs–Marangoni mechanism.

### 478 **3.2.2 Behavior of interfaces under *in vitro* gastric digestion**

479 Once the single and mixed interfacial layers formation was achieved, these were subjected to *in vitro* gastric  
480 lipolysis using the OCTOPUS system and according to the INFOGEST protocol (Brodkorb et al., 2019).  
481 These conditions included an acidic pH (3), the presence of electrolytes, and the inclusion of a relevant  
482 gastric lipase with an activity of 60 U/mL (tributylin based).

483 **Single interfaces:** In Figure 3A-B, the kinetics of interfacial tension are shown after CP and TW80 single  
484 interfaces were subjected to *in vitro* gastric conditions (yellow triangles). Specifically for the CP interfacial  
485 layer (Figure 3A), a very fast decrease was observed in the first minutes of gastric digestion which can be  
486 linked to the adsorption of gastric lipase at the interface. Gastric lipase quickly adsorbed into the defects  
487 present in the CP interfacial film, compressing the interfacial layer. This was also observed for other  
488 biopolymers, such as milk proteins (Mackie et al., 2001; Maldonado-Valderrama et al., 2013). Additionally,  
489 a competitive adsorption phenomenon could have occurred between CP and gastric lipase resulting in the  
490 desorption of the biopolymer from the interface. Afterwards, a more gradual reduction in interfacial tension  
491 was observed, reflecting the production of surface-active lipolysis products (e.g. FFAs and MAGs).  
492 Regarding the interfacial elastic modulus, this property decreased in magnitude from 82 to around 29 mN/m  
493 indicating a loss of the elasticity (Figure 4B). If this latter value was compared with the elastic modulus  
494 after digesting an oil-water interface without emulsifiers (29 mN/m) (Figure 5), then it can be deduced that

495 the interfacial layer at the end of the gastric digestion was mainly composed of lipolysis products. This  
496 means that CP was possibly totally displaced from the interface after 2 hours of *in vitro* gastric digestion.  
497 The CP removal most likely followed the orogenic displacement mechanism, but in this case, the surfactants  
498 (e.g. FFAs and MAGs) were endogenously produced through the hydrolysis of the oil phase. Gastric lipase  
499 and lipolysis products are more surface-active than CP molecules, and possibly caused their removal from  
500 the interface. The desorption step, showed no changes in interfacial tension and interfacial elastic moduli.  
501 This could be explained by the water insoluble character of the lipolysis products of high-oleic sunflower  
502 oil, which accumulate at the interface (Pafumi et al., 2002). In absence of bile salts, these lipolysis products  
503 cannot be removed from the interface and thus are not solubilized in the form of mixed micelles  
504 (Macierzanka et al., 2019; Maldonado-Valderrama et al., 2011). The digestive behavior of this interface  
505 was also similar as compared to the fast and extensive lipolysis behavior observed for the CP-based  
506 emulsion in Section 3.1.2.

507 A completely different scenario occurred for the TW80 interfacial layer under *in vitro* gastric digestion  
508 conditions. As observed in Figure 3B, the TW80 film blocked gastric lipase adsorption, and consequently,  
509 a negligible extent of lipid digestion took place. This behavior was also observed after comparing the final  
510 interfacial tension values of the TW80 interfacial layer before and after *in vitro* gastric digestion (Figure  
511 4A). Moreover, the change in interfacial elastic modulus of the initial TW80 film was very similar to the  
512 one after the digestion step which confirmed that the fluid nature of the TW80 film was maintained.  
513 Therefore, the more surface active TW80 and highly mobile TW80 film restricted the access of enzymes  
514 possibly by Gibbs-Marangoni effects upon deformation of interfacial films (Mackie et al., 2001). In other  
515 words, gastric lipase was not capable to compete for the interface with the more surface active TW80  
516 molecules which rapidly occupied the available interfacial area. This is the reason why very limited lipid  
517 hydrolysis was observed when *in vitro* digesting TW80-based emulsions as discussed in Section 3.1.2. The  
518 desorption phase is difficult to interpret as the TW80 should desorb as the interface is depleted. Conversely,  
519 the interfacial tension remains unchanged after subphase exchange with water. This suggests the presence

520 of irreversibly adsorbed compounds at the interfacial layer. The composition of this final interface is  
521 difficult to interpret as many phenomena might be overlapping; the forced dilution of bulk solution along  
522 with desorption of TW80, solubilization, residual gastric digestion as gastric lipase occupies available space  
523 at the interface, and others.

524 **Mixed interfaces:** Two distinct interfacial tension kinetics and interfacial rheology behaviors during *in*  
525 *vitro* gastric digestion were observed for the single interfacial layers of CP or TW80. In case of mixed  
526 interfacial layers, their kinetics of interfacial tension followed an intermediate behavior compared to the  
527 ones of CP and TW80 single interfacial layers. These kinetics highly depended on the TW80 concentration  
528 employed to form the mixed interfaces as observed in Figure 3C-D. In case of the low TW80 concentration  
529 (0.00625%), the interfacial tension kinetics were similar to the kinetics of a single CP film. This finding is  
530 more clear when comparing the decrease in interfacial tension magnitude before and after *in vitro* digestion  
531 between a single CP film (difference of around 5 mN/m) versus the mixed interface formed with the low  
532 TW80 concentration (difference of around 5 mN/m) (Figure 4A). This differential decrease in interfacial  
533 tension indicates that a similar extent of lipid hydrolysis was reached. However, the more progressive  
534 decrease of interfacial tension during the first minutes of *in vitro* digestion for the mixed interface compared  
535 to the CP single interface was an interesting difference observed from Figures 3A and 3C. For the mixed  
536 interface, the presence of adsorbed TW80 domains at the CP interface modulated the adsorption of gastric  
537 lipase. In this aspect, there was probably a competitive adsorption phenomenon between gastric lipase and  
538 CP molecules taking place. These latter findings may explain the lag-phase encountered during the *in vitro*  
539 gastric digestion of the emulsion stabilized by 1% CP and 0.00625% TW80 (Section 3.1.2). Regarding the  
540 interfacial elastic modulus (Figure 4B), this mixed interface became less elastic as the interconnected  
541 interfacial CP film is partially disrupted by TW80 and/or lipolytic products, presenting a lower magnitude  
542 after *in vitro* digestion (24 mN/m). If the elastic modulus of the single CP and the mixed interface with a  
543 low TW80 concentration after digestion are compared, they were rather similar, yet the one of the mixed  
544 interface was slightly lower. This is possibly because the interface also contained TW80 regions which

545 disrupted the elastic network and hence, decreased the interfacial elastic modulus. Moreover, the formation  
546 of these rather complex interfaces could be responsible for the complex trends observed during the  $\zeta$ -  
547 potential measurements for this mixed system (Table 1). The desorption phase reflected the desorption of  
548 TW80 as the interfacial tension slightly increased. The parallel increase in dilatational elasticity revealed  
549 the presence of lipolysis products anchored at the interface already.

550 The digestion of the mixed interfaced formed using the high TW80 concentration (0.1%) presented a  
551 behavior closer to the one of a single TW80 interface digestion. This is also consistent with findings  
552 regarding the evolution of the  $\zeta$ -potential (Table 1). As observed in Figure 3D, there was a limited  
553 adsorption of gastric lipase, and consequently, a slow decrease in the interfacial tension which can be  
554 interpreted as a low lipid hydrolysis extent. As mentioned in Section 3.3.1, the mixed interfacial layer  
555 formed with the 0.1% TW80 solution presented large regions of adsorbed surfactant while possibly only  
556 few CP molecules remained anchored at the interface. During *in vitro* digestion, gastric lipase probably had  
557 limited access to the interface since the defects in the CP film were already largely occupied by TW80  
558 molecules. Thus, the enzyme most likely competed for the interface with the small fraction of remaining  
559 CP. Under these conditions, a small amount of gastric lipase could adsorb onto the interface, eventually  
560 resulting in a low lipolysis extent. This low extent was also evidenced in Figure 4A, where the differential  
561 interfacial tension before and after *in vitro* digestion was lower than 2 mN/m. With respect to the interfacial  
562 dilatational rheology, Figure 4B shows an elastic modulus of around 15 mN/m, which is somewhat higher  
563 than the one of the interface before *in vitro* digestion (11 mN/m). This possibly means that the interface  
564 was composed of a significant fraction of TW80 molecules as well as some lipolysis products. In another  
565 interesting interfacial study, an interfacial layer covered by TW80 completely inhibited lipid digestion by  
566 HGL. Only in presence of bile salts that removed TW80 from the interface, HGL could initiate the  
567 hydrolysis process (Gargouri et al., 1986). The desorption phase could also reflect the desorption of TW80  
568 as the interfacial tension slightly raised for the mixed systems. This was accompanied by an increase of the  
569 dilatational elasticity that relates to the presence of lipolysis products anchored at the interface. The values

570 reached at this final desorption again serve as prove of the formation of a mixed interfacial layer that  
571 allowed with a fine-tune lipid digestibility.

## 572 **4. Conclusions**

573 This study presented new insight into emulsions stabilized by binary mixed interfaces and their lipid  
574 digestion kinetics evaluation under *in vitro* gastric conditions. All emulsions showed a relatively good to  
575 excellent physical stability during *in vitro* gastric digestion. Therefore, it was hypothesized that lipid  
576 digestion mainly depended on the interfacial composition. The addition of TW80 to CP-based emulsions  
577 permitted the modulation of the lipolysis kinetics as a function of TW80 concentration. A marked lag-phase  
578 was present in the emulsions stabilized by CP and 0.1% TW80. Both the rate and extent of gastric lipid  
579 hydrolysis was decreased by incrementing the TW80 concentration during emulsion preparation. A  
580 competitive adsorption phenomenon was possibly the main driving force for the modulation of lipid  
581 digestion kinetics. Next to this, hypotheses linked to the lipolysis behavior of these emulsions were tested  
582 in a separate experiment consisting of the formation and *in vitro* gastric digestion of interfacial layers.  
583 Overall, it can be claimed that the *in vitro* gastric digestion behaviors of single versus mixed interfacial  
584 layers were analogous to the trends observed for the digestions of their respective o/w emulsions. Two very  
585 distinct interfacial tension kinetics during digestion were observed when single layers of CP or TW80 were  
586 exposed to *in vitro* gastric conditions. When both CP and TW80 were incorporated to form mixed interfacial  
587 layers, intermediate kinetics of gastric lipase adsorption and lipolysis were observed as function of TW80  
588 concentration. This interfacial study confirmed that the competitive adsorption phenomenon (e.g. orogenic  
589 displacement) was the determining factor for lipid hydrolysis of emulsions stabilized by CP and/or TW80,  
590 proving that interfacial design can allow steering of lipolysis kinetics of emulsions. Emulsions stabilized  
591 by mixed interfaces showed a promising tailored lipid digestibility in the gastric phase, but more research  
592 should be conducted to also modulate lipid digestion in the small intestinal phase.

593 **Corresponding authors**

594 **During submission process:**

595 Marcos R. Infantes-Garcia. Laboratory of Food Technology, KU Leuven.

596 Email: [marcos.infantes@kuleuven.be](mailto:marcos.infantes@kuleuven.be)

597 **During post-publication:**

598 Tara Grauwet. Laboratory of Food Technology, KU Leuven.

599 Email: [tara.grauwet@kuleuven.be](mailto:tara.grauwet@kuleuven.be)

600 **Funding**

601 Marcos R. Infantes-Garcia is a Doctoral Researcher funded by the Research Foundation Flanders (FWO -  
602 Grant No. 1S03318N). Sarah H.E. Verkempinck is a Postdoctoral Researcher funded by the Research  
603 Foundation Flanders (FWO - Grant no. 1222420N). The authors also acknowledge the financial support of  
604 the Internal Funds KU Leuven. Julia Maldonado-Valderrama and Teresa Del Castillo-Santaella  
605 acknowledge financial support from Ministerio de Ciencia, Innovación y Universidades-FEDER (RTI2018-  
606 101309-B-C21 and PID2020-116615RA-I00) and from Consejería de Economía, Conocimiento, Empresas  
607 y Universidad-ERDF (SOMM17/6109/UGR). Interfacial characterization experiments were financially  
608 supported by INFOGEST and INRAE through an international research secondment (STSM-2021-004).

609 **Acknowledgement**

610 The authors acknowledge Lipolytech (France) for providing rabbit gastric lipase employed in this research.

611 **Declaration of interests**

612 The authors of this work declare no conflict of interests.

## 613 **References**

- 614 Aguilera-Garrido, A., del Castillo-Santaella, T., Galisteo-González, F., José Gálvez-Ruiz, M., &  
615 Maldonado-Valderrama, J. (2021). Investigating the role of hyaluronic acid in improving curcumin  
616 bioaccessibility from nanoemulsions. *Food Chemistry*, *351*, 129301.  
617 <https://doi.org/10.1016/J.FOODCHEM.2021.129301>
- 618 Bağ, A., & Podgórska, W. (2016). Interfacial and surface tensions of toluene/water and air/water systems  
619 with nonionic surfactants Tween 20 and Tween 80. *Colloids and Surfaces A: Physicochemical and*  
620 *Engineering Aspects*, *504*, 414–425. <https://doi.org/10.1016/J.COLSURFA.2016.05.091>
- 621 Berton-Carabin, C., & Schroën, K. (2019). Towards new food emulsions: designing the interface and  
622 beyond. *Current Opinion in Food Science*, *27*, 74–81. <https://doi.org/10.1016/j.cofs.2019.06.006>
- 623 Bourlieu, C., Ménard, O., Bouzerzour, K., Mandalari, G., Macierzanka, A., Mackie, A. R., Dupont, D., &  
624 Enard, O. (2014). Specificity of Infant Digestive Conditions: Some Clues for Developing Relevant  
625 In Vitro Models. *Critical Reviews in Food Science and Nutrition*, *54*, 1427–1457.  
626 <https://doi.org/10.1080/10408398.2011.640757>
- 627 Bouyer, E., Mekhloufi, G., Rosilio, V., Grossiord, J. L., & Agnely, F. (2012). Proteins, polysaccharides,  
628 and their complexes used as stabilizers for emulsions: Alternatives to synthetic surfactants in the  
629 pharmaceutical field? *International Journal of Pharmaceutics*, *436*(1–2), 359–378.  
630 <https://doi.org/10.1016/J.IJPHARM.2012.06.052>
- 631 Brodkorb, A., Egger, L., Alming, M., Alvito, P., Assunção, R., Ballance, S., Bohn, T., Bourlieu-  
632 Lacanal, C., Boutrou, R., Carrière, F., Clemente, A., Corredig, M., Dupont, D., Dufour, C.,  
633 Edwards, C., Golding, M., Karakaya, S., Kirkhus, B., Le Feunteun, S., ... Recio, I. (2019).  
634 INFOGEST static in vitro simulation of gastrointestinal food digestion. *Nature Protocols*, *14*(4),  
635 991–1014. <https://doi.org/10.1038/s41596-018-0119-1>

- 636 Cabrerizo-Vílchez, M. A., Wege, H. A., Holgado-Terriza, J. A., & Neumann, A. W. (1999).  
637 Axisymmetric drop shape analysis as penetration Langmuir balance. *Review of Scientific*  
638 *Instruments*, 70(5), 2438. <https://doi.org/10.1063/1.1149773>
- 639 Chang, Y., & McClements, D. J. (2016). Influence of emulsifier type on the in vitro digestion of fish oil-  
640 in-water emulsions in the presence of an anionic marine polysaccharide (fucoidan): Caseinate, whey  
641 protein, lecithin, or Tween 80. *Food Hydrocolloids*, 61, 92–101.  
642 <https://doi.org/10.1016/j.foodhyd.2016.04.047>
- 643 Corstens, M. N., Osorio Caltenco, L. A., de Vries, R., Schroën, K., & Berton-Carabin, C. C. (2017).  
644 Interfacial behaviour of biopolymer multilayers: Influence of in vitro digestive conditions. *Colloids*  
645 *and Surfaces B: Biointerfaces*, 153, 199–207. <https://doi.org/10.1016/j.colsurfb.2017.02.019>
- 646 Couédelo, L., Amara, S., Lecomte, M., Meugnier, E., Monteil, J., Fonseca, L., Pineau, G., Cansell, M.,  
647 Carrière, F., Michalski, M. C., & Vaysse, C. (2015). Impact of various emulsifiers on ALA  
648 bioavailability and chylomicron synthesis through changes in gastrointestinal lipolysis. *Food &*  
649 *Function*, 6(5), 1726–1735. <https://doi.org/10.1039/C5FO00070J>
- 650 Dickinson, E. (2011). Mixed biopolymers at interfaces: Competitive adsorption and multilayer structures.  
651 *Food Hydrocolloids*, 25(8), 1966–1983. <https://doi.org/10.1016/J.FOODHYD.2010.12.001>
- 652 Gargouri, Y., Pieroni, G., Riviere, C., Saunier, J.-F., Lowe, P. A., Sarda, L., & Verger, R. (1986).  
653 Kinetic assay of human gastric lipase on short- and long-chain triacylglycerol emulsions.  
654 *Gastroenterology*, 91(4), 919–925. [https://doi.org/10.1016/0016-5085\(86\)90695-5](https://doi.org/10.1016/0016-5085(86)90695-5)
- 655 Gomes, A., Costa, A. L. R., & Cunha, R. L. (2018). Impact of oil type and WPI/Tween 80 ratio at the oil-  
656 water interface: Adsorption, interfacial rheology and emulsion features. *Colloids and Surfaces B:*  
657 *Biointerfaces*, 164, 272–280. <https://doi.org/10.1016/J.COLSURFB.2018.01.032>

658 Grundy, M. M. L., Abrahamse, E., Almgren, A., Alminger, M., Andres, A., Ariëns, R. M. C., Bastiaan-  
659 Net, S., Bourlieu-Lacanal, C., Brodkorb, A., Bronze, M. R., Comi, I., Couëdelo, L., Dupont, D.,  
660 Durand, A., El, S. N., Grauwet, T., Heerup, C., Heredia, A., Infantes Garcia, M. R., ... Carrière, F.  
661 (2021). INFOGEST inter-laboratory recommendations for assaying gastric and pancreatic lipases  
662 activities prior to in vitro digestion studies. *Journal of Functional Foods*, 82, 104497.  
663 <https://doi.org/10.1016/j.jff.2021.104497>

664 Guzmán, E., Llamas, S., Maestro, A., Fernández-Peña, L., Akanno, A., Miller, R., Ortega, F., & Rubio, R.  
665 G. (2016). Polymer-surfactant systems in bulk and at fluid interfaces. In *Advances in Colloid and*  
666 *Interface Science* (Vol. 233, pp. 38–64). Elsevier. <https://doi.org/10.1016/j.cis.2015.11.001>

667 Humerez-Flores, J. N., Verkempinck, S. H. E., De Bie, M., Kyomugasho, C., Van Loey, A. M.,  
668 Moldenaers, P., & Hendrickx, M. E. (2022). Understanding the impact of diverse structural  
669 properties of homogalacturonan rich citrus pectin-derived compounds on their emulsifying and  
670 emulsion stabilizing potential. *Food Hydrocolloids*, 125, 107343.  
671 <https://doi.org/10.1016/J.FOODHYD.2021.107343>

672 Humerez-Flores, J. N., Verkempinck, S. H. E., Kyomugasho, C., Moldenaers, P., Van Loey, A. M., &  
673 Hendrickx, M. E. (2021). Modified Rhamnogalacturonan-Rich Apple Pectin-Derived Structures:  
674 The Relation between Their Structural Characteristics and Emulsifying and Emulsion-Stabilizing  
675 Properties. *Foods 2021*, Vol. 10, Page 1586, 10(7), 1586. <https://doi.org/10.3390/FOODS10071586>

676 Infantes-Garcia, M. R., Verkempinck, S. H. E., Gonzalez-Fuentes, P. G., Hendrickx, M. E., & Grauwet,  
677 T. (2021). Lipolysis products formation during in vitro gastric digestion is affected by the emulsion  
678 interfacial composition. *Food Hydrocolloids*, 110, 106163.  
679 <https://doi.org/10.1016/j.foodhyd.2020.106163>

680 Infantes-Garcia, M. R., Verkempinck, S. H. E., Guevara-Zambrano, J. M., Andreoletti, C., Hendrickx, M.  
681 E., & Grauwet, T. (2020). Enzymatic and chemical conversions taking place during in vitro gastric

682 lipid digestion: The effect of emulsion droplet size behavior. *Food Chemistry*, 326, 126895.  
683 <https://doi.org/10.1016/j.foodchem.2020.126895>

684 Infantes-Garcia, M. R., Verkempinck, S. H. E., Guevara-Zambrano, J. M., Hendrickx, M. E., & Grauwet,  
685 T. (2021). Development and validation of a rapid method to quantify neutral lipids by NP-HPLC-  
686 charged aerosol detector. *Journal of Food Composition and Analysis*, 102, 104022.  
687 <https://doi.org/10.1016/j.jfca.2021.104022>

688 Infantes-Garcia, M. R., Verkempinck, S. H. E., Saadi, M. R., Hendrickx, M. E., & Grauwet, T. (2022).  
689 Towards understanding the modulation of in vitro gastrointestinal lipolysis kinetics through  
690 emulsions with mixed interfaces. *Food Hydrocolloids*, 124, 107240.  
691 <https://doi.org/10.1016/J.FOODHYD.2021.107240>

692 Karupaiah, T., & Sundram, K. (2007). Effects of stereospecific positioning of fatty acids in triacylglycerol  
693 structures in native and randomized fats: a review of their nutritional implications. *Nutrition &*  
694 *Metabolism*, 4, 16. <https://doi.org/10.1186/1743-7075-4-16>

695 Klinkesorn, U., & McClements, D. J. (2009). Influence of chitosan on stability and lipase digestibility of  
696 lecithin-stabilized tuna oil-in-water emulsions. *Food Chemistry*, 114(4), 1308–1315.  
697 <https://doi.org/10.1016/j.foodchem.2008.11.012>

698 Kyomugasho, C., Gwala, S., Christiaens, S., Jamsazzadeh Kermani, Z., Van Loey, A. M., Grauwet, T., &  
699 Hendrickx, M. E. (2017). Pectin nanostructure influences pectin-cation interactions and in vitro-  
700 bioaccessibility of Ca<sup>2+</sup>, Zn<sup>2+</sup>, Fe<sup>2+</sup> and Mg<sup>2+</sup>-ions in model systems. *Food Hydrocolloids*, 62,  
701 299–310. <https://doi.org/10.1016/J.FOODHYD.2016.07.030>

702 Layer, P., & Keller, J. (2005). Gastric lipase and pancreatic exocrine insufficiency. *Clinical*  
703 *Gastroenterology and Hepatology*, 3(1), 25–27. [https://doi.org/10.1016/S1542-3565\(04\)00607-X](https://doi.org/10.1016/S1542-3565(04)00607-X)

704 Li, Y., & McClements, D. J. (2014). Modulating lipid droplet intestinal lipolysis by electrostatic  
705 complexation with anionic polysaccharides: Influence of cosurfactants. *Food Hydrocolloids*, 35,  
706 367–374. <https://doi.org/10.1016/j.foodhyd.2013.06.011>

707 Lindquist, S., & Hernell, O. (2010). Lipid digestion and absorption in early life: an update. *Current*  
708 *Opinion in Clinical Nutrition and Metabolic Care*, 13(3), 314–320.  
709 <https://doi.org/10.1097/MCO.0b013e328337bbf0>

710 Macierzanka, A., Sancho, A. I., Mills, E. N. C., Rigby, N. M., & Mackie, A. R. (2009). Emulsification  
711 alters simulated gastrointestinal proteolysis of  $\beta$ -casein and  $\beta$ -lactoglobulin. *Soft Matter*, 5(3), 538–  
712 550. <https://doi.org/10.1039/B811233A>

713 Macierzanka, A., Torcello-Gómez, A., Jungnickel, C., & Maldonado-Valderrama, J. (2019). Bile salts in  
714 digestion and transport of lipids. *Advances in Colloid and Interface Science*, 274, 102045.  
715 <https://doi.org/10.1016/j.cis.2019.102045>

716 Mackie, A. R., Gunning, A. P., Ridout, M. J., Wilde, P. J., & Patino, J. R. (2001). In situ measurement of  
717 the displacement of protein films from the air/water interface by surfactant. *Biomacromolecules*,  
718 2(3), 1001–1006. <https://doi.org/10.1021/bm015540i>

719 Mackie, A. R., Gunning, A. P., Wilde, P. J., & Morris, V. J. (1999). Orogenic displacement of protein  
720 from the air/water interface by competitive adsorption. *Journal of Colloid and Interface Science*,  
721 210(1), 157–166. <https://doi.org/10.1006/jcis.1998.5941>

722 Mackie, A. R., Gunning, A. P., Wilde, P. J., & Morris, V. J. (2000). Orogenic displacement of protein  
723 from the oil/water interface. *Langmuir*, 16(5), 2242–2247. <https://doi.org/10.1021/la990711e>

724 Maldonado-Valderrama, J. (2019). Probing in vitro digestion at oil–water interfaces. *Current Opinion in*  
725 *Colloid & Interface Science*, 39, 51–60. <https://doi.org/10.1016/J.COCIS.2019.01.004>

726 Maldonado-Valderrama, J., Fainerman, V. B., Gálvez-Ruiz, M. J., Martín-Rodríguez, A., Cabrerizo-  
727 Vílchez, M. A., & Miller, R. (2005). Dilatational Rheology of  $\beta$ -Casein Adsorbed Layers at  
728 Liquid–Fluid Interfaces. *Journal of Physical Chemistry B*, *109*(37), 17608–17616.  
729 <https://doi.org/10.1021/JP050927R>

730 Maldonado-Valderrama, J., & Patino, J. M. R. (2010). Interfacial rheology of protein–surfactant mixtures.  
731 *Current Opinion in Colloid & Interface Science*, *15*(4), 271–282.  
732 <https://doi.org/10.1016/J.COCIS.2009.12.004>

733 Maldonado-Valderrama, J., Terriza, J. A. H., Torcello-Gómez, A., & Cabrerizo-Vílchez, M. A. (2013). In  
734 vitro digestion of interfacial protein structures. *Soft Matter*, *9*(4), 1043–1053.  
735 <https://doi.org/10.1039/c2sm26843d>

736 Maldonado-Valderrama, J., Wilde, P., Macierzanka, A., & Mackie, A. (2011). The role of bile salts in  
737 digestion. *Advances in Colloid and Interface Science*, *165*(1), 36–46.  
738 <https://doi.org/10.1016/j.cis.2010.12.002>

739 McClements, D. J. (2016). *Food Emulsions. Principles, Practices, and Techniques* (Third). CRC  
740 Press/Taylor & Francis Group. <https://doi.org/10.1201/9781420029581.ch9>

741 McClements, D. J. (2018). Enhanced delivery of lipophilic bioactives using emulsions: a review of major  
742 factors affecting vitamin, nutraceutical, and lipid bioaccessibility. *Food & Function*, *9*(1), 22–41.  
743 <https://doi.org/10.1039/C7FO01515A>

744 McClements, D. J., & Jafari, S. M. (2018). Improving emulsion formation, stability and performance  
745 using mixed emulsifiers: A review. *Advances in Colloid and Interface Science*, *251*, 55–79.  
746 <https://doi.org/10.1016/j.cis.2017.12.001>

747 Neckebroeck, B., Verkempinck, S. H. E., Vaes, G., Wouters, K., Magnée, J., Hendrickx, M. E., & Van  
748 Loey, A. M. (2020). Advanced insight into the emulsifying and emulsion stabilizing capacity of  
749 carrot pectin subdomains. *Food Hydrocolloids*, *102*. <https://doi.org/10.1016/j.foodhyd.2019.105594>

750 Ngouémazong, E. D., Christiaens, S., Shpigelman, A., Van Loey, A., & Hendrickx, M. (2015). The  
751 Emulsifying and Emulsion-Stabilizing Properties of Pectin: A Review. *Comprehensive Reviews in*  
752 *Food Science and Food Safety*, *14*(6), 705–718. <https://doi.org/10.1111/1541-4337.12160>

753 Pafumi, Y., Lairon, D., de la Porte, P. L., Juhel, C., Storch, J., Hamosh, M., & Armand, M. (2002).  
754 Mechanisms of inhibition of triacylglycerol hydrolysis by human gastric lipase. *The Journal of*  
755 *Biological Chemistry*, *277*(31), 28070–28079. <https://doi.org/10.1074/jbc.M202839200>

756 Scheuble, N., Lussi, M., Geue, T., Carrière, F., & Fischer, P. (2016). Blocking Gastric Lipase Adsorption  
757 and Displacement Processes with Viscoelastic Biopolymer Adsorption Layers. *Biomacromolecules*,  
758 *17*(10), 3328–3337. <https://doi.org/10.1021/acs.biomac.6b01081>

759 Schmidt, U. S., Schütz, L., & Schuchmann, H. P. (2017). Interfacial and emulsifying properties of citrus  
760 pectin: Interaction of pH, ionic strength and degree of esterification. *Food Hydrocolloids*, *62*, 288–  
761 298. <https://doi.org/10.1016/J.FOODHYD.2016.08.016>

762 Singh, H., & Ye, A. (2013). Structural and biochemical factors affecting the digestion of protein-  
763 stabilized emulsions. *Current Opinion in Colloid & Interface Science*, *18*(4), 360–370.  
764 <https://doi.org/10.1016/J.COCIS.2013.04.006>

765 Singh, H., Ye, A., & Horne, D. (2009). Structuring food emulsions in the gastrointestinal tract to modify  
766 lipid digestion. *Progress in Lipid Research*, *48*(2), 92–100.  
767 <https://doi.org/10.1016/j.plipres.2008.12.001>

768 Troise, A. D., Fogliano, V., & Madadlou, A. (2020). Tailor it up! How we are rolling towards designing  
769 the functionality of emulsions in the mouth and gastrointestinal tract. *Current Opinion in Food*  
770 *Science*, 31, 126–135. <https://doi.org/10.1016/J.COFS.2020.06.002>

771 Verkempinck, S. H. E., Kyomugasho, C., Salvia-Trujillo, L., Denis, S., Bourgeois, M., Van Loey, A. M.,  
772 Hendrickx, M. E., & Grauwet, T. (2018). Emulsion stabilizing properties of citrus pectin and its  
773 interactions with conventional emulsifiers in oil-in-water emulsions. *Food Hydrocolloids*, 85(3),  
774 144–157. <https://doi.org/10.1016/j.foodhyd.2018.07.014>

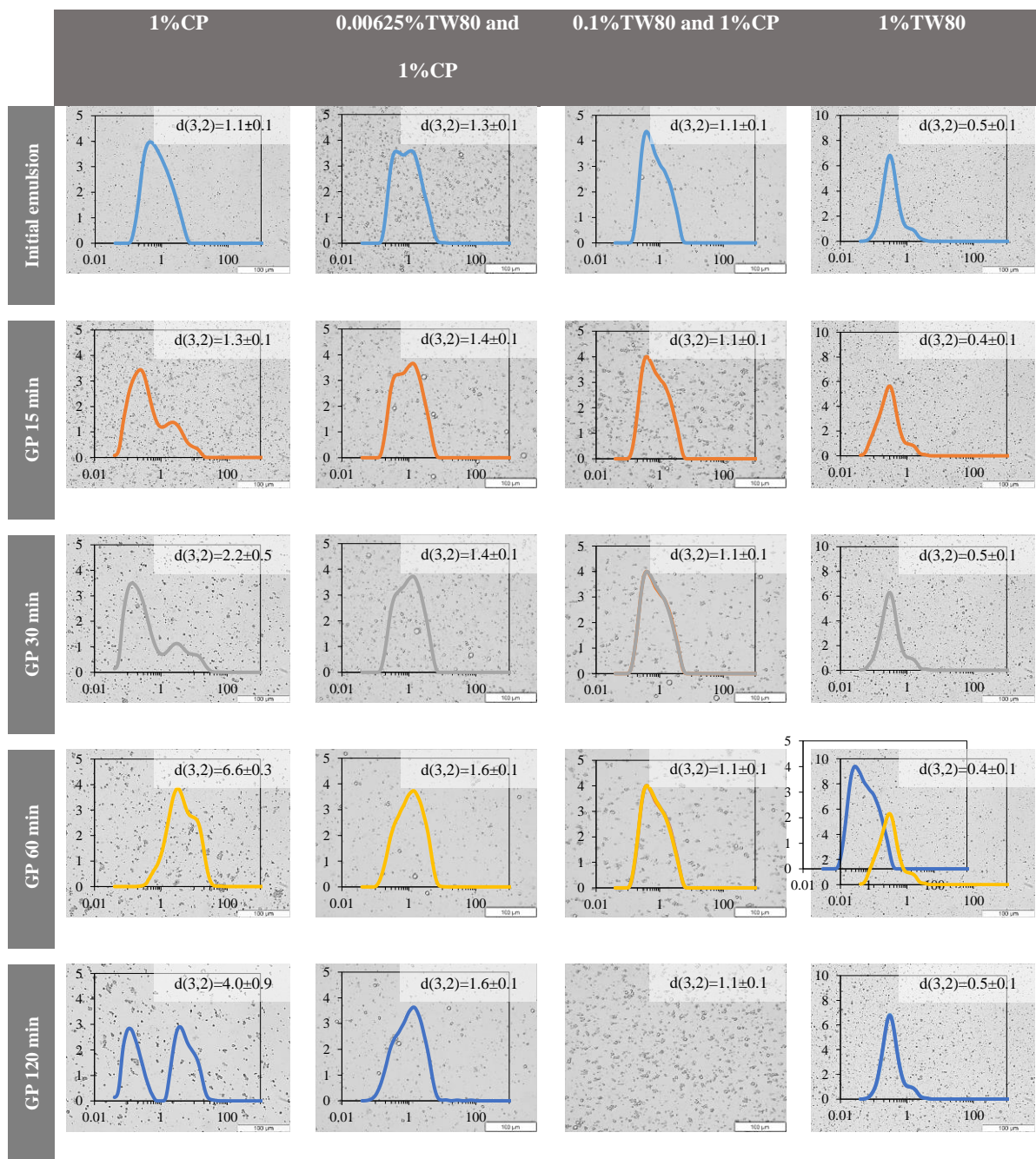
775 Verkempinck, S. H. E., Salvia-Trujillo, L., Denis, S., Van Loey, A. M., Hendrickx, M. E., & Grauwet, T.  
776 (2018). Pectin influences the kinetics of in vitro lipid digestion in oil-in-water emulsions. *Food*  
777 *Chemistry*, 262, 150–161. <https://doi.org/10.1016/j.foodchem.2018.04.082>

778 Verkempinck, S. H. E., Salvia-Trujillo, L., Moens, L. G., Charleer, L., Van Loey, A. M., Hendrickx, M.  
779 E., & Grauwet, T. (2018). Emulsion stability during gastrointestinal conditions effects lipid  
780 digestion kinetics. *Food Chemistry*, 246, 179–191.  
781 <https://doi.org/10.1016/J.FOODCHEM.2017.11.001>

782 Wei, R., Zhao, S., Zhang, L., Feng, L., Zhao, C., An, Q., Bao, Y., Zhang, L., & Zheng, J. (2021). Upper  
783 digestion fate of citrus pectin-stabilized emulsion: An interfacial behavior perspective.  
784 *Carbohydrate Polymers*, 264, 118040. <https://doi.org/10.1016/J.CARBPOL.2021.118040>

785 Wulff-Pérez, M., Gálvez-Ruíz, M. J., de Vicente, J., & Martín-Rodríguez, A. (2010). Delaying lipid  
786 digestion through steric surfactant Pluronic F68: A novel in vitro approach. *Food Research*  
787 *International*, 43(6), 1629–1633. <https://doi.org/10.1016/j.foodres.2010.05.006>

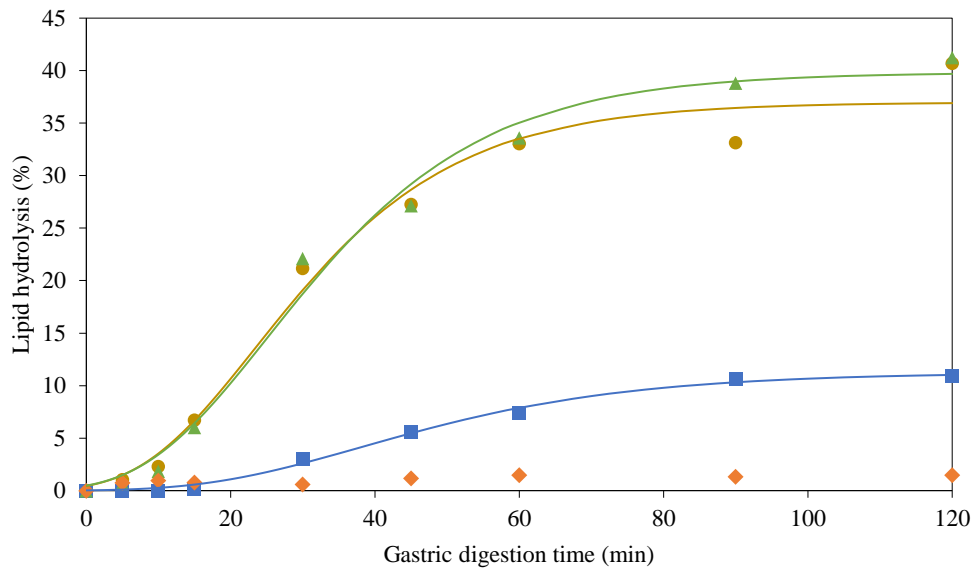
788 Zwietering, M. H., Jongenburger, I., Rombouts, F. M., & Van't Riet, K. (1990). Modeling of the bacterial  
789 growth curve. *Applied and Environmental Microbiology*, 56(6), 1875–1881.  
790 <https://doi.org/10.1128/aem.56.6.1875-1881.1990>



792

793 **Figure 1.** Effect of *in vitro* gastric conditions (GP) on the particle size distribution (PSD), average surface-based  
 794 particle size  $d(3,2)$  and microstructure of o/w emulsions stabilized by mixed interfaces composed of citrus pectin  
 795 (CP) and/or Tween 80 (TW80). Scale bars in the micrographs represent 100  $\mu\text{m}$ . X-axis and Y-axis of PSD graphs  
 796 indicate the oil droplet diameter ( $\mu\text{m}$ ) and surface fraction (%), respectively.

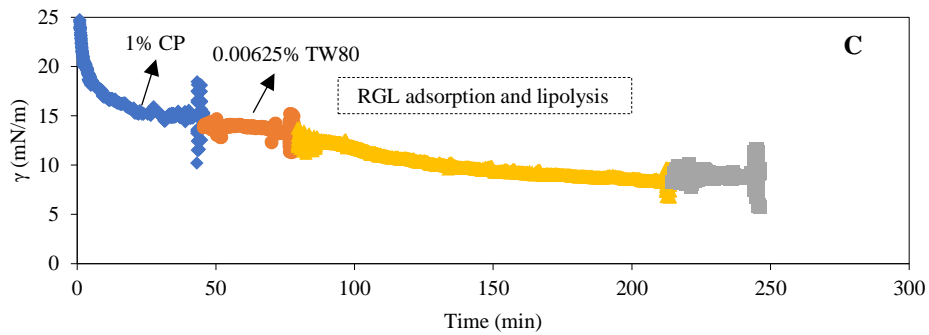
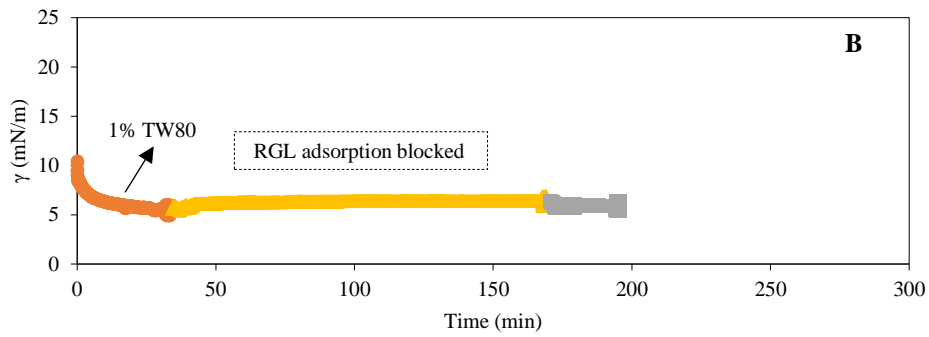
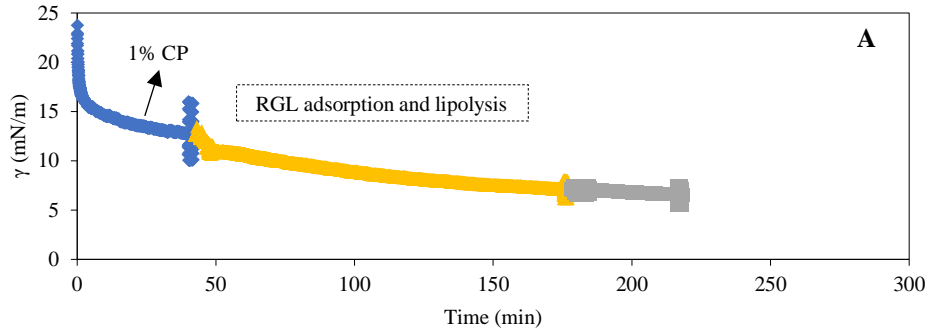
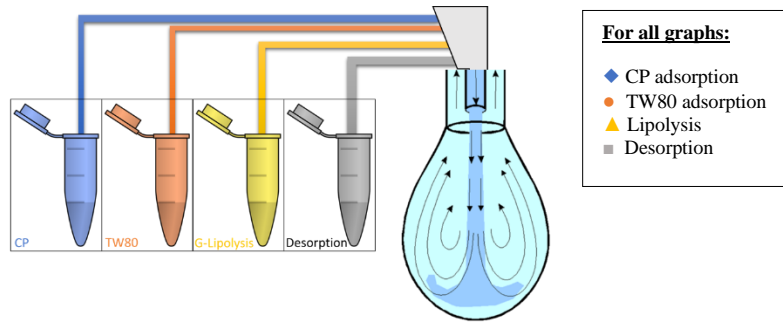
797

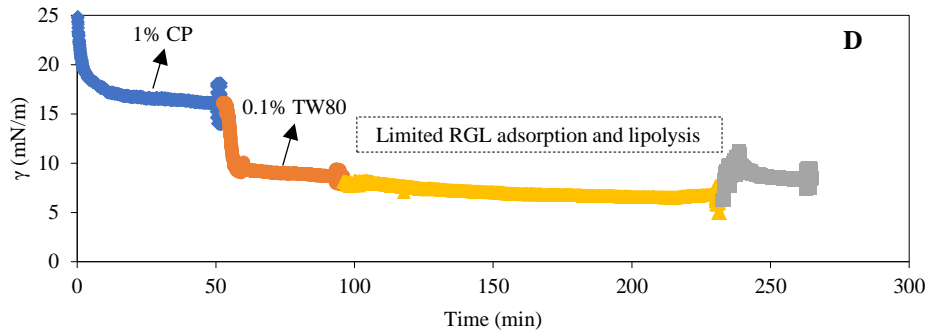


798

799 **Figure 2.** Modulation of the lipid hydrolysis percentage of emulsions stabilized by single and mixed interfaces  
800 containing citrus pectin (CP) and/or Tween 80 (TW80) and subjected to *in vitro* gastric digestion: (▲) 1% CP, (●) 1%  
801 CP and 0.00625% TW80, (■) 1% CP and 0.1% TW80, and (◆) 1% TW80. Symbols represent the experimental  
802 analyte concentrations, while solid lines represent model curves fitted with the modified Gompertz equation.

803

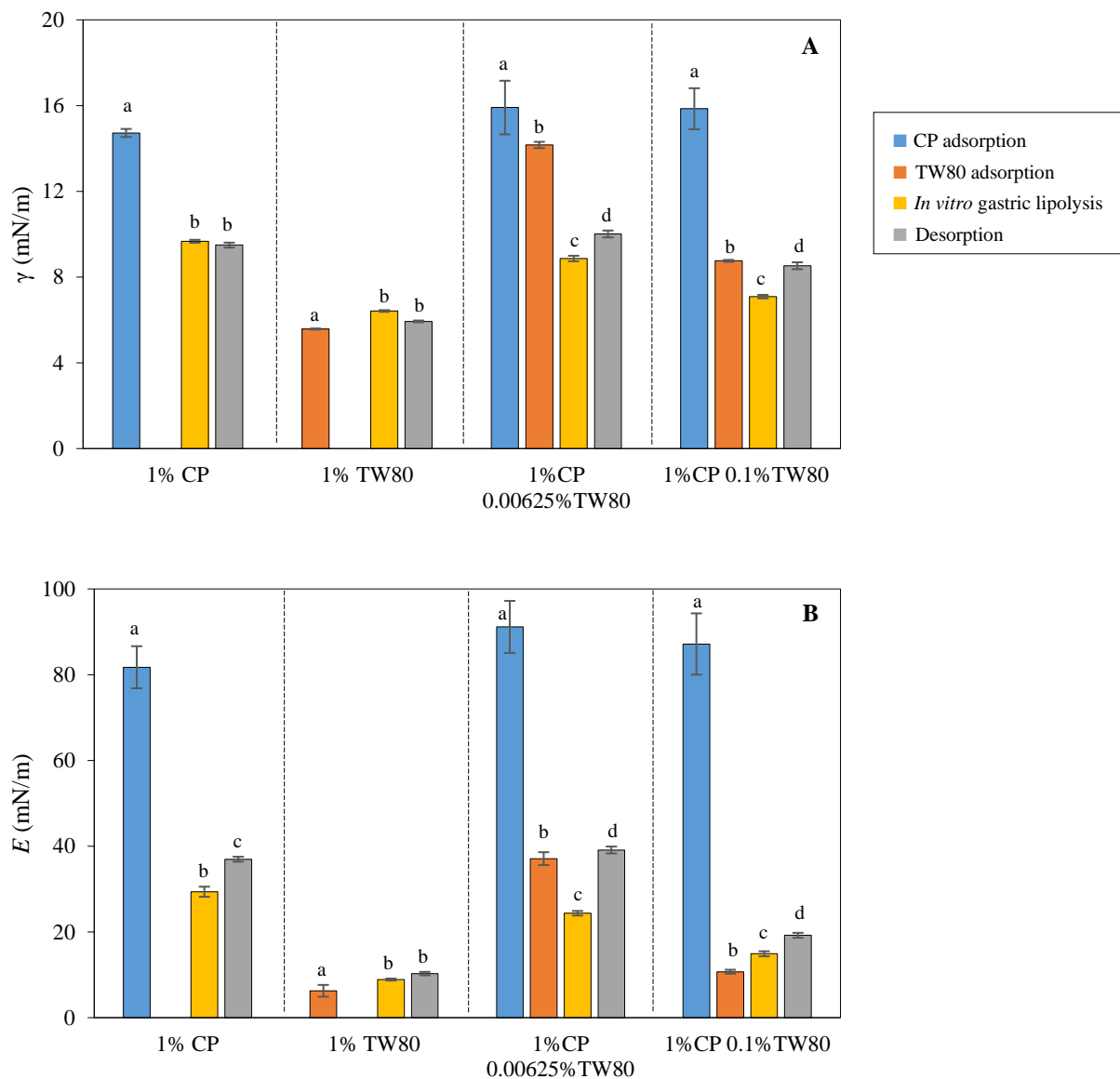




804

805 **Fig. 3.** Interfacial tension ( $\gamma$ ) kinetics of immersed aqueous phase droplets in high-oleic sunflower oil measured with  
 806 the OCTOPUS system (modified pendant drop technique) for single interfaces formed after placing solutions of (A)  
 807 1% citrus pectin (CP), (B) 1% Tween 80 (TW80), and mixed interfaces formed after sequentially injecting solutions  
 808 of (C) 1% CP and then 0.00625% TW80, and (D) 1% CP and then 0.1% TW80. The formed interfaces were subjected  
 809 to *in vitro* gastric digestion (pH 3, rabbit gastric lipase activity (RGL) of 60 U/mL) followed by a desorption step  
 810 (injection of ultrapure water). Oscillatory values (vertical lines) of the interfacial tension at the end of each stage (e.g.  
 811 interface formation or digestion) correspond to the interfacial rheology measurement.

812



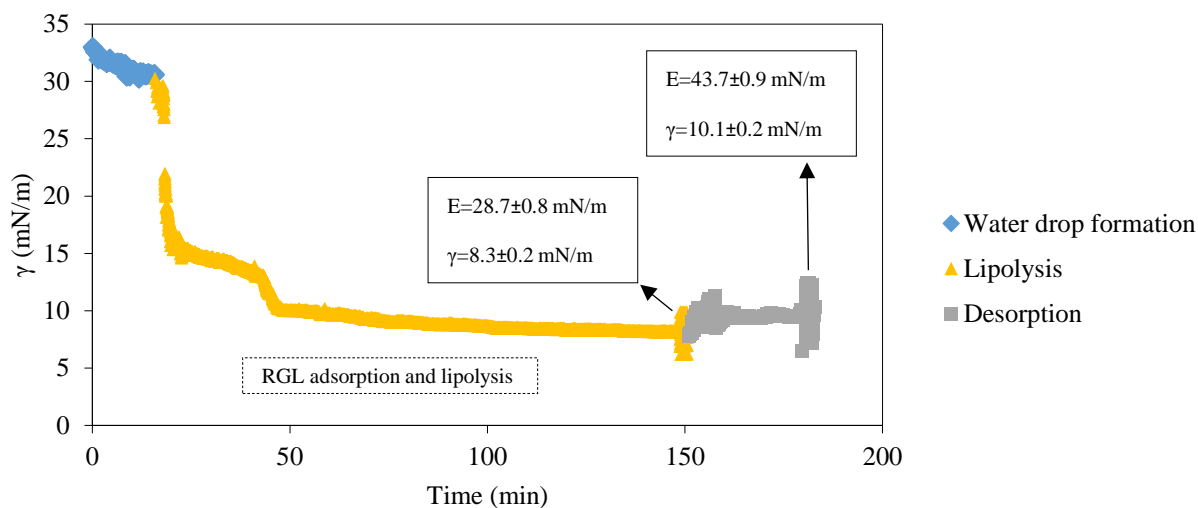
813

814 **Figure 4.** (A) Interfacial tension ( $\gamma$ ) and (B) interfacial dilatational elastic moduli ( $E$ ) of immersed aqueous phase  
 815 droplets in high-oleic sunflower oil at equilibrium measured with the OCTOPUS system (modified pendant drop  
 816 technique) for single interfaces formed after injecting solutions of 1% citrus pectin (CP), 1% Tween 80 (TW80), and  
 817 mixed interfaces formed after subsequently injecting solutions of 1% CP and 0.00625% TW80, and 1% CP and 0.1%  
 818 TW80. The formed interfaces were subjected to *in vitro* gastric digestion (rabbit gastric lipase activity 60 U/mL)  
 819 followed by a desorption step. The oscillation amplitude to determine  $E$  was maintained below 5% variation and the  
 820 oscillation frequency was set to 0.1 Hz. In graph B, the values represent measurements after each

821 adsorption/digestion/desorption step (vertical lines in Figure 3). Different lower case letters indicate significant  
822 differences among each adsorption/digestion/desorption step per interface type using Tukey HSD comparison tests.

823

824



825

826 **Fig. 5.** Interfacial tension ( $\gamma$ ) kinetics and interfacial dilatational elastic moduli (E) of an immersed water drop  
827 in high-oleic sunflower oil subjected to *in vitro* gastric digestion (pH 3, rabbit gastric lipase activity  
828 (RGL) of 60 U/mL) followed by a desorption step, and measured in the OCTOPUS system (modified  
829 pendant drop technique).

830

831

832

833

834

835

836

837

838 **Table 1.**  $\zeta$ -potential of o/w emulsions stabilized by single and mixed interfaces during *in vitro* gastric digestion (GP).  
 839 Different lower case letters indicate significant differences ( $P < 0.05$ ) between different digestion times from the same  
 840 emulsion.

841

Emulsifier concentration in emulsion	Initial emulsion	GP 15 min	GP 30 min	GP 60 min	GP 120 min
1%CP	-20.1 $\pm$ 0.8 <sup>a</sup>	-0.5 $\pm$ 0.1 <sup>b</sup>	1.9 $\pm$ 0.2 <sup>c</sup>	1.7 $\pm$ 0.2 <sup>c</sup>	1.5 $\pm$ 0.2 <sup>c</sup>
1%CP and 0.00625%TW80	-14.1 $\pm$ 0.1 <sup>a</sup>	-6.7 $\pm$ 0.2 <sup>b</sup>	-6.7 $\pm$ 1.9 <sup>b</sup>	-7.0 $\pm$ 0.4 <sup>b</sup>	-6.8 $\pm$ 0.3 <sup>b</sup>
1%CP and 0.1 %TW80	-6.8 $\pm$ 0.3 <sup>a</sup>	-0.8 $\pm$ 0.5 <sup>b</sup>	-0.4 $\pm$ 0.3 <sup>b</sup>	-0.8 $\pm$ 0.1 <sup>c</sup>	-2.0 $\pm$ 0.1 <sup>d</sup>
1%TW80	-1.4 $\pm$ 0.1 <sup>a</sup>	-2.0 $\pm$ 0.2 <sup>b</sup>	-1.8 $\pm$ 0.2 <sup>b</sup>	-1.9 $\pm$ 0.2 <sup>b</sup>	-1.8 $\pm$ 0.6 <sup>b</sup>

842

843

844 **Table 2.** Estimated parameters of the percentage of lipid hydrolysis using the modified Gompertz equation of  
 845 emulsions stabilized by citrus pectin (CP) and/or Tween 80 (TW80) subjected to *in vitro* gastric digestion. The  
 846 parameter  $t_{lag}$  is the estimated lag time (min),  $k$  is the estimated hydrolysis rate constant ( $\text{min}^{-1}$ ), and  $H_f$  is the estimated  
 847 final hydrolysis extent (%) as indicated in equation 3. Different lower case letters indicate significant differences  
 848 among each parameter estimate according to their confidence intervals (95%).

849

	Estimated lipid hydrolysis parameters		
	$t_{lag}$ (min)	$k$ ( $\text{min}^{-1}$ )	$H_f$ (%)
1%CP	8.2 $\pm$ 2.3 <sup>a</sup>	0.86 $\pm$ 0.09 <sup>a</sup>	39.8 $\pm$ 1.5 <sup>a</sup>
1%CP and 0.00625%TW80	7.7 $\pm$ 2.8 <sup>a</sup>	0.86 $\pm$ 0.12 <sup>a</sup>	36.9 $\pm$ 1.7 <sup>a</sup>
1%CP and 0.1 %TW80	16.8 $\pm$ 2.1 <sup>b</sup>	0.19 $\pm$ 0.02 <sup>b</sup>	11.3 $\pm$ 0.4 <sup>b</sup>

850

851